Origin of the dispersion limit in the preparation of Ni(Co)Mo/Al2O3 and Ni(Co)Mo/TiO2 HDS oxidic precursors

Carole Lamonier, Deana Soogund, Jean Mazurelle, Pascal Blanchard, Denis Guillaume, Edmond Payen

Title
A.B. Editor et al. (Editors)

Origin of the dispersion limit in the preparation of Ni(Co)Mo/Al_2O_3 and Ni(Co)Mo/TiO_2 HDS oxidic precursors

Carole Lamonier[1], Deana Soogund[1], Jean Mazurelle[1], Pascal Blanchard[1], Denis Guillaume[2] and Edmond Payen[1]

[1]*Unité de Catalyse et Chimie du solide, UMR 8181, Université des Sciences et Technologies de Lille, Bâtiment C3, 59655 Villeneuve d'Ascq, France*
[2]*Institut Français du Pétrole, Direction Catalyse et Séparation, IFP-Lyon, BP3, 69390 Vernaison, FRANCE*

Conventional alumina and titania oxidic precursors have been characterized by Raman spectroscopy after maturation, drying and calcination. The evolution of the impregnating solution has been followed and the nature of the precipitates has been determined. After impregnation of alumina 6molybdoaluminate entities (well dispersed or not) are characterized for both the NiMo and CoMo based solids. At high Mo loading, the formation of a CoMo oxyhydroxide that yields bulk cobalt molybdate upon calcination is also observed. In counterpart on TiO_2 surface of the NiMo precursor, the formation of 6molybdonickelate leading to bulk nickel molybdate upon calcination is observed. The formation of well defined phases i.e. $CoMoO_4$ and $NiMoO_4$ was not observed on respectively titania and alumina supports, but well dispersed polyoxomolybdate was characterized at the same Mo loading.

1. Introduction

HDS is a catalytic process generally performed with Co(Ni)Mo/Al_2O_3 system, the active phase of which consists of well-dispersed MoS_2 nanocrystallittes decorated with Co or Ni atoms [1]. These phases are obtained by sulfidation of an oxidic precursor that is generally prepared by incipient wetness impregnation of an alumina support with ammonium heptamolybdate (AHM) and cobalt or nickel nitrate solutions. However the dispersion of the supported oxides is limited at high metal loading and improvement of the catalytic performances requires a more complete understanding of the genesis of the oxidic precursor. A better comprehension of the exact origin of this limit of good dispersion is therefore necessary. It is now clearly admitted that during the impregnation of an alumina, some aluminum atoms are extracted from the

support and yield 6molybdoaluminate $(AlMo_6H_6O_{24})^{3-}$ ($AlMo_6$) entities. These Anderson heteropolystructures are well dispersed and/or precipitated on this support according to the Mo loading [2]. This work therefore deals with the extension of this dissolution/precipitation concept to the preparation of Ni(Co)Mo catalysts. Extension of the study to titania supported oxidic precursor will also be considered as it has been shown that TiO_2 [3] supported MoS_2 catalysts present 3 to 5 times higher hydrodesulphurization and hydrogenation activities than alumina supported ones with an equivalent Mo loading per nm^2 [4]. However the synergy between Co(Ni) and Mo in the TiO_2 supported catalyst appears to be lower than in the alumina supported one [5].
In this work, we will first study the stability of conventional CoMo and NiMo impregnating solutions. NiMo and CoMo oxidic precursors have been prepared by incipient wetness impregnation of γ alumina and titania supports. They will be characterized at each step of the preparation by Raman spectroscopy. Characterization results will be discussed by reference to the chemistry of the impregnating solution which will allow us to explain the differences between CoMo and NiMo based catalysts.

2. Experimental

2.1. Raman spectroscopy

The Raman spectra of the samples, maintained at room temperature, were recorded using a Raman microprobe (Infinity from Jobin - Yvon), equipped with a photodiode array detector. The exciting laser source was the 532 nm line of a Nd-YAG laser. The wavenumber accuracy was 2 cm^{-1}

2.2. Oxidic precursors preparation

The samples were prepared by incipient wetness impregnation of the support with (AHM + cobalt nitrate) and (AHM + nickel nitrate) aqueous solutions. The Mo concentration was adjusted taking into account alumina and titania pore volumes that are respectively 0.8 and 0.4 $mL.g^{-1}$ in order to prepare catalyst with Mo loadings corresponding to 10, 14 and 16 MoO_3 wt % on alumina. On titania the maximum content on molybdenum that can be obtained is 10 MoO_3 wt %. Note that in this case the TiO_2 supported solid has 3,5 Mo atoms per nm^2 as obtained for a Al_2O_3 supported one with a molybdenum content of 16 MoO_3 wt %. After two hours of maturation, the solids were dried under air at 95°C and then calcined at 500°C for 4 h under oxygen. The samples will be designated according to the starting solution and the support as follows XNiMoy/TiO_2, X being the molybdenum loading expressed as a weight percentage of MoO_3 and y being the Co(Ni)/Mo ratio.

3. Results and Discussion

3.1. Stability of the Co or Ni based impregnating solutions

The stability of impregnating solutions has been studied by LRS at different Mo concentrations. The Co/Mo and Ni/Mo ratio studied are 0.17 and 0.5. From a catalytic point of view 0.5 is the optimum value [6] whereas the former one (0.17) is the ratio corresponding to the stoechiometry of the Anderson molybdocobaltate or Anderson molybdonickelate $[XMo_6H_6O_{24}]^{n-}$ heteropolyanion. Figure 1 shows the Raman spectra of these CoMo and NiMo solutions before precipitation. They exhibit the characteristic lines of the heptamolybdate anions in solution with the main lines at 942, 895 and 364 cm^{-1}, the line at 1050 cm^{-1} corresponding to nitrate anions. Whereas the Mo and CoMo solutions are relatively stable without any precipitation before several hours, a precipitation is rapidly observed for the NiMo based solutions, whatever the metal loading and the Ni/Mo ratio.

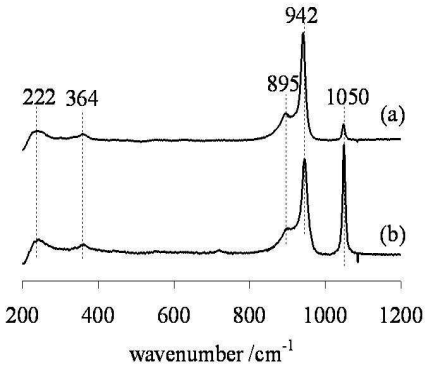

Fig. 1 : Raman spectra before precipitation of (a) CoMo solution and (b) NiMo solution

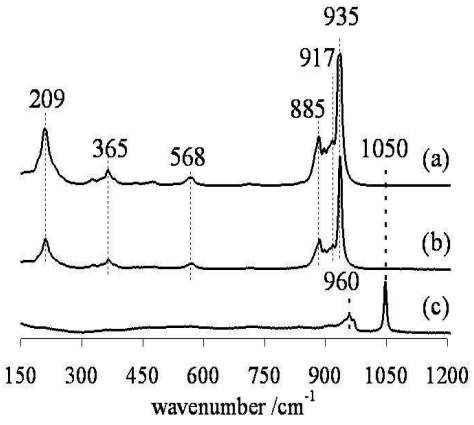

Fig. 2 : Raman spectra of (a) precipitate from a NiMo solution (b) $NiMo_6H_6O_{24}(NH_4)_3$ Anderson solid and (c) the NiMo filtered solution

Figure 2 presents the Raman spectra of the precipitate and of the filtered Ni based solution. The Raman spectrum of the filtered solution with a main line at 960 cm^{-1} is assigned by reference to literature data [7] to condensed isopolymolybdate as $[Mo_8O_{26}]^{4-}$. Such a formation is in agreement with the

decrease of the pH observed upon addition of nickel nitrate in the HMA solution. Indeed for a Ni/Mo ratio equal to 0.5 the pH solution decreases from 5.7 until 3.5. The precipitate obtained by filtration is sky-blue and its Raman spectrum is similar to the Anderson anion $[NiMo_6H_6O_{24}]^{4-}$ as shown in figure 2 in which the spectrum of the ammonium salt is also reported. The main features characteristic of the Mo-O_{2t} (where t stands for terminal) and of the Mo-O-Ni bonds appear respectively at 935 and 568 cm^{-1}.
Precipitation of a CoMo solution is only observed after several hours. The Raman spectrum of the precipitate (not reported here) clearly exhibits the features of HMA for Co/Mo=0.17 whereas for the highest Co/Mo=0.5 the spectrum is also characteristic of condensed isopolymolybdate species in agreement with the pH decrease of the solution. This study indicates that no Anderson heteropolyanion is formed. Indeed some discrepancies appeared in the literature concerning the existence of the molybdocobaltate $[CoMoO_{24}H_6]^{4-}$, HPA in which the oxidation state of the central heteroatom is +2. Indeed La Ginestra [8] reported its formation whereas Nomiya [9] proposed later that the Co(II) should be excluded from the Anderson family and that such structure should enter into another category of heteropolyanion, this compound being likely $[Co(H_2O)_{6-x}(Mo_7O_{24})]^{4-}$ as proposed by Malik and al. [10]. Thus in impregnating solution containing cobalt, our results indicate that a cobalt Anderson based heteropolyanion, with cobalt at the oxidation state 2+, is not formed in our preparation conditions. At high metal loading a precipitation occurs and the precipitate corresponds to HMA and/or $Mo_8O_{26}(NH_4)_4$ mixture according to the pH solution whereas in the case of nickel the $[NiMo_6H_6O_{24}]^{4-}$ HPA is most probably formed in solution but due to the low solubility of its ammonium salt a precipitation occurs.

3.2. Deposition on alumina support

3.2.1. Unpromoted alumina supported oxidic precursors

It has been shown through a Raman, NMR and Mo K-edge EXAFS spectroscopic study, that upon impregnation of alumina with AHM solution a decomposition occurs with extraction of aluminium atoms of the support [11,12] and their inclusion in the Anderson HPA $AlMo_6O_{24}H_6^{3-}$ [3,13]. These $AlMo_6$ entities are well dispersed and/or precipitated on this support according to the Mo loading [3]. For an incipient wetness impregnation, the highest Mo loading is governed by the maximum solubility of the AHM and therefore it depends on the pore volume of the alumina. However as the solubility of $AlMo_6$ ammonium salt is lower than the AHM one, the precipitation of this salt is observed at high Mo loading.

3.2.2. Alumina supported promoted oxidic precursors

Raman spectra of the promoted matured (not reported here) and dried samples exhibit the features of well dispersed $AlMo_6$ entities for NiMo (figure 3) and CoMo (figure 4 (b)) based solids. For the NiMo solids, whatever the Mo loading, 10, 14 or 16 MoO_3 wt %, the Raman spectra only present a main line at 948 cm^{-1} and a line around 563 cm^{-1} in the domain of Mo-O-Al vibrations, attesting the homogeneity of the surface species.

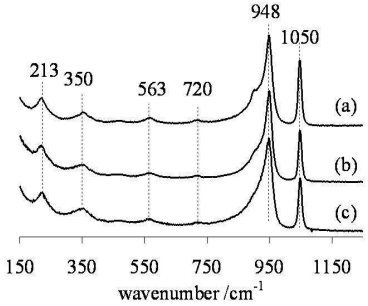

Fig. 3 : Raman spectra after drying of (a) 16NiMo0.5/Al_2O_3 (b) 14NiMo0.5/Al_2O_3 and (c) 10NiMo0.5/Al_2O_3

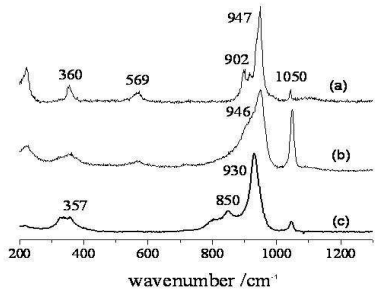

Fig. 4 : Raman spectra of CoMo0.5/Al_2O_3 after drying (a) 16CoMo0.5/Al_2O_3, (b) and (c) 14CoMo0.5/Al_2O_3 (different particles)

Heterogeneities are highlighted at high Mo loading for the CoMo based precursor. Indeed other features in figure 4 (c) (930 and 850 cm^{-1}) are also observed that have been assigned to the formation of a mixed CoMo oxohydroxide phase whereas the precipitation of the $AlMo_6$ ammonium salt is noticed in these CoMo at high Mo loading (16MoO_3 wt %), figure 4 (a). Upon calcination this heterogeneity is confirmed. After transfer in the air the well dispersed $AlMo_6$ entities are restored. But the Raman spectrum of the calcined CoMo solid (not reported here) also exhibits, after transfer in wet air, the line characteristic of the (a)$CoMoO_4$ phase (940 and 818 cm^{-1}) that should originates from the CoMo oxyhydroxyde precipitate as it is not observed at lower Mo loading for which no heterogeneity was evidenced on the dried solid. For a 16CoMo/Al_2O_3 catalyst MoO_3 phase is detected with the lines at 995 and 819 cm^{-1} its formation originates upon calcination from the $(NH_4)_3AlMo_6O_{24}H_6$ crystallites deposited at the alumina surface after drying. As far as the NiMo dried solid are concerned, no heterogeneity appears even at high Mo loading and after calcination whatever the molybdenum content the Raman spectra (not reported here) show only the main line characteristic of the

well dispersed polymolybdate phase (a large line at 950 cm^{-1}). The absence of MoO_3 and/or $NiMoO_4$ phase after calcination confirms the good dispersion of molybdenum.

3.3. Deposition on titania support

3.3.1. Unpromoted titania supported oxidic precursors

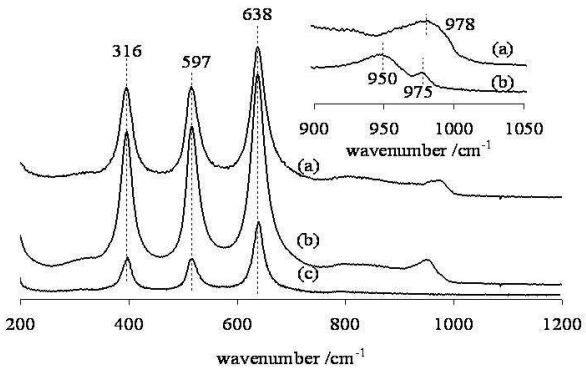

Fig. 5 : Raman spectra of (a) 10Mo/TiO_2 after calcination (b) 10Mo/TiO_2 after drying and (c) TiO_2 support

The Raman spectra of unpromoted sample in the dried and calcined state are presented on figure 8 together with the spectrum of the support. In agreement with literature data [14], the spectrum of the titania support (figure 5 (c)) exhibits the three well resolved lines at 316 (B_{1g}), 597 (A_{1g}) and 638 cm^{-1} (E_g) that are also observed on the oxidic precursor spectra. At the dried step for the unpromoted solid (figure 5 (b)) the AHM features are no longer observed and the broad line at 950 cm^{-1} shows the formation of a well-dispersed polymolybdate phase whose structure is not yet clearly established. This phase has also been reported by Ng and Gulari [4] and defined as octahedrally coordinated polymeric Mo species. In this spectrum (see the zoom) line is noticed at 975 cm^{-1} that could be assigned to a protonated form of $Mo_8O_{26}^{4-}$ [7] the formation of which can be explained by the acidity of TiO_2 support. Upon calcination (figure 5 (a)) this line becomes greater and the Raman spectrum is shifted towards higher wavenumbers but no MoO_3 phase is detected, attesting the good metal dispersion.

3.3.2. Promoted titania supported oxidic precursors

Raman spectra of $NiMo/TiO_2$ and $CoMo/TiO_2$ in the dried and calcined state are reported figure 6 in which only the 700-1200 spectral range is presented. Whatever the state of the solid, we note a high similarity between the spectra of $CoMo/TiO_2$ and Mo/TiO_2 (figure 5). Unlike the $CoMo/Al_2O_3$, in $CoMo/TiO_2$ solids cobalt does not interact strongly with the support to form well defined bulk or subsurface Co-TiO_2 phase. However literature data indicates that as Mo support interaction is lower on titania than on alumina,

addition of cobalt suppresses the formation of MoO_3 and leads to the formation of cobalt molybdate [5,15]. But controversy about the role of titania can be found. Indeed Ng and Gulari described TiO_2 as a strongly interacting support [4]. In our case neither $CoMoO_4$ nor MoO_3 features are observed in the Raman spectra after calcination (figure 6 (a)). The 10CoMo/TiO_2 catalyst has the same Mo coverage (3,5 atoms of Mo/nm^2) as the alumina one on which the formation of cobalt molybdate is observed. We can therefore consider that its absence on the CoMo/TiO_2 one is due to the homogeneity of deposition during the impregnation. The formation of CoMo oxyhydroxide is not noticed on titania for a same metal concentration of the impregnating solution. The NiMo system differs from the CoMo one. After drying, the Raman spectrum of the 10NiMo/TiO_2 (figure 6(e)) exhibits the characteristic lines of the $NiMo_6$ entities (936, 920 and 887 cm^{-1}). After calcination Raman lines at 960 and 913 cm^{-1} (figure 6(c)) indicate the formation of (b)$NiMoO_4$ species according

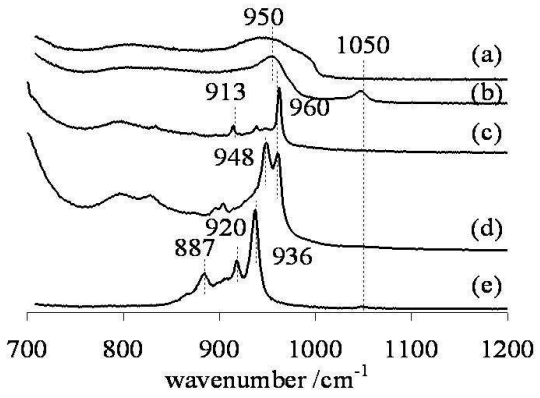

Fig. 6 : Raman spectra of TiO_2 supported oxidic precursors (a) 10CoMo0.5/TiO_2 after calcination, (b) 10CoMo0.5/TiO_2 after drying, (c) and (d) 10NiMo0.5/TiO_2 after calcination (different particles) and (e) 10NiMo0.5/TiO_2 after drying

to the literature references [14]. Moreover a well dispersed molybdate phase is also noticed on the calcined NiMo based precursor, corresponding to the line at 948 cm^{-1} (figure 6(d)). These results are in agreement with UV-DRS study of Wei *et al* [16] in which the authors deduced that in NiMo/TiO_2-Al_2O_3 catalysts the Ni^{2+} ions were located in an octahedral environment and yield $NiMoO_4$-like phase upon calcination.

4. Conclusion

For alumina CoMo and NiMo supported oxidic precursors the same trend is observed. Raman analysis evidences the formation of a well dispersed $AlMo_6$ phase after the maturation and drying steps whichever the promoter atom. However at high Mo loading other phases are observed for CoMo based

solids such a CoMooxyhydroxide and $AlMo_6$ ammonium precipitate. They yield respectively $CoMoO_4$ and MoO_3 phases upon calcination. In the case of NiMo solids, molybdenum and nickel remain well dispersed on alumina from the maturation to the calcination step even at high metal loading.
On titania the behavior of nickel and cobalt solids is rather different. After drying, on one hand we observed with NiMo solids the formation of $NiMo_6$ precipitate whereas on the other hand no heteropolyanionic phase $Co^{II}Mo_6$ is formed, isopolymolydate phase being well dispersed on CoMo solids. These differences are reflected in the calcined state. After calcination, a $NiMoO_4$ phase is noticed besides a dispersed molybdate phase for NiMo oxidic precursor. This study clearly shows that the chemistry of the impregnating solutions and the solubility of the ammonium $AlMo_6$ and $NiMo_6$ entities determine the nature of the species formed at the surface of the precursors at high Mo loading and subsequently determine the limit of dispersion of the metal atoms. Improvement of catalytic performances can be obtained by using impregnating solutions without ammonium counter ion. We therefore propose the use of a new precursor, a cobalt salt of $[Co_2Mo_{10}H_4O_{38}]^{6-}$ that has been proved as an efficient starting material [17].

REFERENCES

1. Topsoe, H.; Candia, R.; Topsoe, N. Y.; Clausen, B. S. *Bull. Soc.Chim. Bel.* **1984,** *93*, 783-806.
2. Le Bihan, L.; Blanchard, P.; Fournier, M.; Grimblot, J.; Payen, E. *J. Chem. Soc., Far. Trans.* **1998,** *94*, 937-940.
3. Okamoto, Y.; Ochiai, K.; Kawano, M.; Kobayashi, K.; Kubota, T. *Appl. Catal., A: General* **2002,** *226*, 115-127..
4 Ng, K. Y. S.; Gulari, E. *J. Catal.* **1985,** *92*, 340-54.
5. Ramirez, J.; Fuentes, S.; Diaz, G.; Vrinat, M.; Breysse, M.; Lacroix, M. *Appl.Catal.* **1989,** *52*, 211-23.
6. Rob van Veen, J. A.; Gerkema, E.; Van der Kraan, A. M.; Knoester, A. *J. Chem. Soc., Far. Trans. Communications* **1987**, 1684-6.
7. Wang, L.; Hall, W. K. *J. Catal.* **1980,** *66*, 251-5.
8. La Ginestra, A.; Giannetta, F.; Fiorucci, P. *Gazzetta Chimica Italiana* **1968,** *98*, 1197-212.
9. Nomiya, K.; Takahashi, T.; Shirai, T.; Miwa, M. *Polyhedron* **1987,** *6*, 213-18.
10. Malik, A.; Zubaili, S. A.; Khan, S. *J. Chem. Soc. Dalt. transaction* **1977**, 1049.
11. Payen, E.; Plazenet, G.; Martin, C.; Lamonier, C.; Lynch, J.; Harle, V. *Stu. Surf. Sci. Cata.* **2002,** *143*, 141-148.
12. Plazenet, G.; Payen, E.; Lynch, J.; Rebours, B. *J. Phys. Chem. B* **2002,** *106*, 7013-7028.
13. Carrier, X.; Lambert, J. F.; Che, M. *J. Am. Chem. Soc.* **1997,** *119*, 10137-10146.
14. Dzwigaj, S.et al, *Appl. Catal., B* **2003,** *41*, 181-191.
15. Leliveld, R. G.; Van Dillen, A. J.; Geus, J. W.; Koningsberger, D. C. *J. Catal.* **1997,** *171*, 115-129.
16. Wei, Z. B.; Yan, W.; Zhang, H.; Ren, T.; Xin, Q.; Li, Z. *Appl. Catal., A* **1998,** *167*, 39-48.
17. Lamonier, C.; Martin, C.; Mazurelle, J.; Harlé, V.; Guillaume, D. *Appl. Catal. B, under press* **2006**.